Optical single-angle plane-wave transmittances/reflectances from Schwarzschild objective variable-angle measurements

Thomas K. Gaylord and Gregory R. Kilby

Citation: Rev. Sci. Instrum. **75**, 317 (2004); doi: 10.1063/1.1641160
View online: http://dx.doi.org/10.1063/1.1641160
View Table of Contents: http://rsi.aip.org/resource/1/RSINAK/v75/i2
Published by the American Institute of Physics.

Optical single-angle plane-wave transmittances/reflectances from Schwarzschild objective variable-angle measurements

Thomas K. Gaylord[a] and Gregory R. Kilby
School of Electrical and Computer Engineering, Georgia Institute of Technology, Atlanta, Georgia 30332-0250

(Received 8 September 2003; accepted 15 November 2003)

Photonic crystal structures and other nanoscale and microscale optical structures are centrally important to future device technology. The fundamental infrared single-angle plane-wave experimental characterization of these structures is needed to evaluate the analysis, design, and fabrication progress on these devices. The very small sizes of these devices necessitates focusing the infrared probe light typically with a Schwarzschild reflecting objective. The small spot size inherently requires the large range of incident angles associated with the objective. In this work, a variable-angle measurement method is presented for obtaining the optical single-angle plane-wave transmittances/reflectances. The primary steps in this method are (1) calculating the reference sample single-angle plane-wave transmittance/reflectance, (2) measuring the composite transmittances/reflectances of a reference sample over a range of objective angles of incidence, (3) calculating the intensity-angular-weighting coefficients for the objective using the Moore–Penrose (overdetermined linear equations) matrix inversion technique, (4) measuring the composite transmittances/reflectances of a sample-under-test over a range of objective angles of incidence, and (5) calculating the single-angle plane-wave transmittances/reflectances using the Moore–Penrose matrix inversion technique. [DOI: 10.1063/1.1641160]

I. INTRODUCTION

Optical devices based on photonic crystal structures have the potential to manipulate and control light in many useful ways.[1] These and related nanoscale and microscale optical devices can function as waveguides, right-angle waveguide bends, resonators, input/output couplers, spontaneous emission controllers, light localizers, optical interconnections, etc. Devices may have locally periodic variations in one, two, or three dimensions. Since the first introduction of photonic crystal structures,[2,3] there have been many theoretical papers and fabrication papers published on these important structures. Although a great deal of excellent progress has been made, photonic crystal devices are not yet in wide commercial use. The structures are small and complex. Nonoptimum device performance might be ascribed to shortcomings in analysis, design, fabrication, or a combination of these. There are many uncertainties accompanying the development of these devices. Hence there is a significant need for accurate experimental measurements on the structures that are fabricated. Testing is critical, especially over a range of infrared wavelengths. Only by such measurements can device developers know what they have achieved.

To address the need for measurements over a range of infrared wavelengths, researchers have successfully employed Fourier transform infrared (FTIR) transmission microscopy,[4–9] FTIR reflection microscopy,[6,9–15] optical parametric oscillator (OPO) microscopy,[10,16–19] and carbon dioxide (CO_2) laser microscopy.[20] These investigations have provided many valuable results and insights. In general, these approaches require focusing of the infrared beam. This is typically done with a Schwarzschild reflecting objective which like all objectives produces a range of angles of incidence. Furthermore, unlike a refracting lens, the Schwarzschild reflecting objective produces a (nonzero) minimum as well as a maximum angle of incidence. The range of angles produced by the objective directly determines the angles of incidence that occur in a given measurement made with the objective. A method is needed for obtaining the infrared single-angle plane-wave transmittances/reflectances.

In this article, a variable-angle measurement method is presented for obtaining the optical single-angle plane-wave transmittances/reflectances. First, the operation of the Schwarzschild reflecting objective is described. Then the method is presented. It consists of the following steps: (1) installing a horizontal slit before the objective to limit angles of incidence, (2) calculating the reference sample single-angle plane-wave transmittance/reflectance (e.g., using Fresnel's equations), (3) inserting the reference semiconductor slab sample aligned with the horizontal slit, (4) measuring the composite transmittances/reflectances of a reference sample over a range of objective angles of incidence, (5) calculating the intensity-angular-weighting coefficients for the objective using the Moore–Penrose (overdetermined linear equations) matrix inversion technique, (6) inserting the photonic crystal semiconductor sample aligned with the horizotal slit, (7) measuring the composite transmittances/reflectances of a sample-under-test over a range of objective angles of incidence, and (8) calculating the single-angle plane-wave transmittances/reflectances using the Moore–

[a]Author to whom correspondence should be addressed; electronic mail: tgaylord@ece.gatech.edu

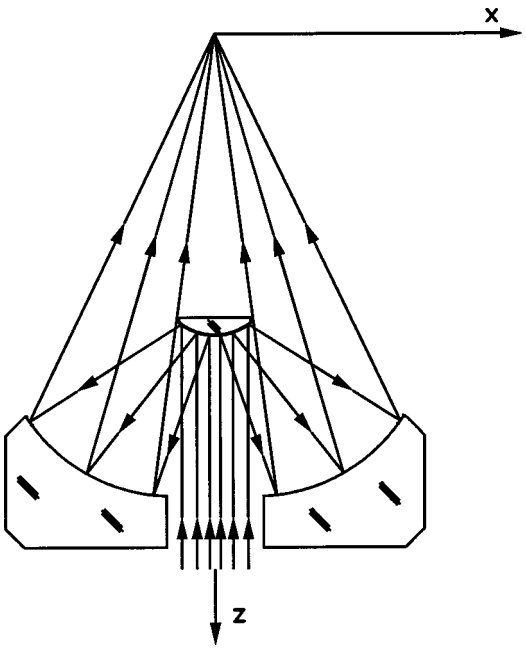

FIG. 1. Optical configuration of Schwarzschild reflecting focusing objective. Light passes through a hole in the primary mirror, is reflected by the secondary mirror, then is reflected by the primary mirror, and brought to a focus as shown.

Penrose matrix inversion technique. In the following sections, each of these steps is described.

II. SCHWARZSCHILD REFLECTING OBJECTIVE

The Schwarzschild reflecting objective produces a range of angles of incidence as shown in Fig. 1. The objective angles incident on the sample range from $-\theta_{\mathrm{ob,max}}$ to $-\theta_{\mathrm{ob,min}}$ and from $+\theta_{\mathrm{ob,min}}$ to $+\theta_{\mathrm{ob,max}}$ as indicated in Fig. 2. These angles include all angles with circular symmetry about the z axis of the objective. Some example commercial Schwarzschild reflecting objectives made by Thermo-Oriel[21] and Ealing[22] are described in Table I. For the measurements described here, a horizontal slit along the x direction is located before the objective. Thus each ray incident on the sample has a wave vector $\mathbf{k}$ lying in the $x-z$ plane. The development presented here is in terms of transmittances. However, a similar procedure applies to the determination of plane-wave reflectances. With the Schwarzschild objective, measured transmittances are integrations (summations) over a range of angles of incidence. From composite angular measurements made with the Schwarzschild objective, it is desired to determine the single-angle plane-wave transmittance, t_j, of the photonic crystal structure where j is the index over the single-angle plane-wave angles of incidence. The measured composite transmittances are represented by T_i where i is the index over angles of the objective axis with respect to the sample, $\theta_{s,i}$. The measured transmittances may be represented as incoherent weighted sums of the plane-wave transmittances t_j. That is,

$$T_i = \sum_j A_{ij} t_j, \tag{1}$$

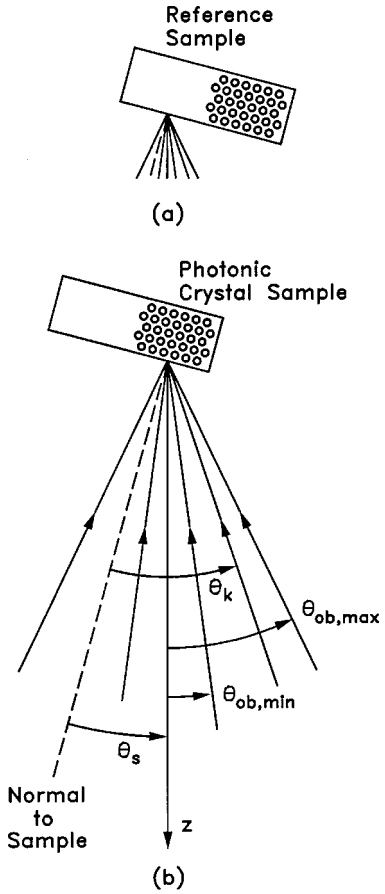

FIG. 2. Light rays from Schwarzschild objective incident (a) upon a reference (or slab) sample and (b) upon a photonic crystal sample. The normal to the sample is at an angle θ_s with respect to the axis of the objective. The minimum and maximum ray angles of the objective are given by $\theta_{\mathrm{ob,min}}$ and $\theta_{\mathrm{ob,max}}$, respectively. An example single-angle plane-wave angle, θ_k, is shown.

where A_{ij} are the weighting coefficients for the plane waves that are present. For a given objective angle with respect to the sample, $\theta_{s,i}$, many plane wave components will be absent and thus the corresponding A_{ij} coefficients will be zero for those components. For the realistic case of the intensity of the incident infrared radiation intensity not being the same for each angle from $-\theta_{\mathrm{ob,max}}$ to $-\theta_{\mathrm{ob,min}}$ and from $+\theta_{\mathrm{ob,min}}$ to $+\theta_{\mathrm{ob,max}}$ then $A_{i,j-1} \neq A_{i,j} \neq A_{i,j+1}$, for each plane-wave angle of incidence for that objective orientation. However, the objective intensity weighting coefficients will not depend on the objective angle with respect to the sample (index i). The coefficients depend only on the infrared beam and the Schwarzschild objective optics and not on how the sample is oriented with respect to the objective. For clarity of presen-

TABLE I. Example commercial Schwarzschild reflecting objectives including their minimum and maximum ray angles.

Manufacturer	Model No.	Magnification	Numerical aperture	$\theta_{\mathrm{ob,min}}$ (deg)	$\theta_{\mathrm{ob,max}}$ (deg)
Thermo-Oriel	13595	15×	0.4	9.8	23.6
Thermo-Oriel	13596	36×	0.5	10.3	30.0
Ealing	25-0514	25×	0.4	9.4	23.5
Ealing	25-0522	36×	0.5	10.0	30.0

tation, the index i (for the objective-sample angle) and the index j (for the single-angle plane wave) are taken to be the value in degrees of those corresponding angles (rather than consecutive integers). Also, the intensity weighting coefficients will be designated by the single subscript j (rather than by two subscripts) with the values in degrees for the case of $i=0$ (normal incidence for objective). Further, to simplify the presentation, a large angular spacing (10°) is used to represent consecutive values of the composite transmittances, the weighting coefficients, and the single-angle plane-wave transmittances. Still further, the Schwarzschild objective used in the development here is assumed to be described by only three weighting coefficients corresponding to $\theta_{\mathrm{ob}}=20°$, 30°, and 40°. For these angles the intensity weighting coefficients are given by $A_{0,20}\equiv a_{20}$, $A_{0,30}\equiv a_{30}$, and $A_{0,40}\equiv a_{40}$. To obtain higher angular resolution in the single-angle plane-wave transmittances, obviously measurements, weighting coefficients, and calculations would need to be obtained at a smaller angular spacing (such as 1°). Note that the maximum angle of objective-sample incidence, $\theta_{s,i}$, is $90°-\theta_{\mathrm{ob,max}}$. At this objective-sample angle of incidence, there are rays at grazing incidence. In some experimental configurations, the mechanical arrangement of the sample and objective will limit the maximum angle of objective-sample incidence to a value lower than this. Using these conventions and facts, the measured composite transmittances, T_i, in terms of the single-angle plane-wave transmittances, t_j, are given by

$$\begin{bmatrix} T_{50} \\ T_{40} \\ T_{30} \\ T_{20} \\ T_{10} \\ T_{0} \\ T_{-10} \\ T_{-20} \\ T_{-30} \\ T_{-40} \\ T_{-50} \end{bmatrix} = \begin{bmatrix} a_{40} & a_{30} & a_{20} & 0 & 0 & 0 & a_{20} & a_{30} & a_{40} & 0 & 0 & 0 & 0 & 0 & 0 & 0 & 0 & 0 & 0 \\ 0 & a_{40} & a_{30} & a_{20} & 0 & 0 & 0 & a_{20} & a_{30} & a_{40} & 0 & 0 & 0 & 0 & 0 & 0 & 0 & 0 & 0 \\ 0 & 0 & a_{40} & a_{30} & a_{20} & 0 & 0 & 0 & a_{20} & a_{30} & a_{40} & 0 & 0 & 0 & 0 & 0 & 0 & 0 & 0 \\ 0 & 0 & 0 & a_{40} & a_{30} & a_{20} & 0 & 0 & 0 & a_{20} & a_{30} & a_{40} & 0 & 0 & 0 & 0 & 0 & 0 & 0 \\ 0 & 0 & 0 & 0 & a_{40} & a_{30} & a_{20} & 0 & 0 & 0 & a_{20} & a_{30} & a_{40} & 0 & 0 & 0 & 0 & 0 & 0 \\ 0 & 0 & 0 & 0 & 0 & a_{40} & a_{30} & a_{20} & 0 & 0 & 0 & a_{20} & a_{30} & a_{40} & 0 & 0 & 0 & 0 & 0 \\ 0 & 0 & 0 & 0 & 0 & 0 & a_{40} & a_{30} & a_{20} & 0 & 0 & 0 & a_{20} & a_{30} & a_{40} & 0 & 0 & 0 & 0 \\ 0 & 0 & 0 & 0 & 0 & 0 & 0 & a_{40} & a_{30} & a_{20} & 0 & 0 & 0 & a_{20} & a_{30} & a_{40} & 0 & 0 & 0 \\ 0 & 0 & 0 & 0 & 0 & 0 & 0 & 0 & a_{40} & a_{30} & a_{20} & 0 & 0 & 0 & a_{20} & a_{30} & a_{40} & 0 & 0 \\ 0 & 0 & 0 & 0 & 0 & 0 & 0 & 0 & 0 & a_{40} & a_{30} & a_{20} & 0 & 0 & 0 & a_{20} & a_{30} & a_{40} & 0 \\ 0 & 0 & 0 & 0 & 0 & 0 & 0 & 0 & 0 & 0 & a_{40} & a_{30} & a_{20} & 0 & 0 & 0 & a_{20} & a_{30} & a_{40} \end{bmatrix} \begin{bmatrix} t_{90} \\ t_{80} \\ t_{70} \\ t_{60} \\ t_{50} \\ t_{40} \\ t_{30} \\ t_{20} \\ t_{10} \\ t_{0} \\ t_{-10} \\ t_{-20} \\ t_{-30} \\ t_{-40} \\ t_{-50} \\ t_{-60} \\ t_{-70} \\ t_{-80} \\ t_{-90} \end{bmatrix}, \quad (2)$$

where the maximum angle of objective-sample incidence has been taken arbitrarily to be 50°. For the objective at normal incidence, $\theta_{s,i}=0$, the corresponding measured transmittance T_0 is the sum of the plane-wave transmittances from $\theta_k=-\theta_{\mathrm{ob,max}}$ to $\theta_k=-\theta_{\mathrm{ob,min}}$ and from $\theta_k=+\theta_{\mathrm{ob,min}}$ to $\theta_k=+\theta_{\mathrm{ob,max}}$. For $\theta_{\mathrm{ob,min}}=20°$ and $\theta_{\mathrm{ob,max}}=40°$ as depicted in Eq. (2), and for the objective at $\theta_{s,i}=+10°$, then measured transmittance T_{10} is the weighted sum of the plane-wave transmittances at −30°, −20°, −10°, +30°, +40°, and +50°.

For symmetric photonic crystal structures, such as the one shown in Fig. 2, positive and negative angles of incidence should produce the same result. Using this, Eq. (2) can be simplified. From symmetry, $t_{10}=t_{-10}$, $t_{20}=t_{-20}$, $t_{30}=t_{-30}$, etc., and so

$$t_j=t_{-j}. \quad (3)$$

Further, objective-sample angles of incidence beyond $\theta_{s,\mathrm{max}}$ are not possible. In practice, the largest angle of plane-wave incidence would be $\theta_{k,\mathrm{max}}$ where

$$\theta_{k,\mathrm{max}}=\theta_{s,\mathrm{max}}+\theta_{\mathrm{ob,max}}. \quad (4)$$

Incidence at and near 90°, as indicated in Eq. (2), may not be possible depending on the particular experimental configuration.

III. COMPOSITE TRANSMITTANCES OF REFERENCE SAMPLE

Initially, a blank reference slab (typically silicon or other semiconductor material) is inserted into the system. The single-angle plane-wave intensity transmittances t_j's are calculated for this slab. This may be done using the Fresnel equations, finite-difference time-domain (FDTD) methods, or other electromagnetic modeling methods. Here, for simplicity, the Fresnel equations are used to calculate the single-

angle plane-wave intensity transmittances t_j's taking into account a single reflection at the entrance surface and at the exit surface of the reference silicon slab. These are designated as "slab" (sl) values, $t_{sl,0}$, $t_{sl,10}$, $t_{sl,20},\ldots,t_{sl,90}$. For TE polarization (electric field perpendicular to the plane of incidence) and TM polarization (magnetic field perpendicular to plane of incidence), the amplitudes of the transmitted fields at the air–semiconductor interface are

$$\left(\frac{E_t}{E_i}\right)_{\text{TE}} = \frac{2n_1\cos\theta_1}{n_1\cos\theta_1 + n_2\cos\theta_2},$$
$$\left(\frac{E_t}{E_i}\right)_{\text{TM}} = \frac{2n_1\cos\theta_1}{n_2\cos\theta_1 + n_1\cos\theta_2}, \tag{5}$$

where $n_1=1$ is the index of air, n_2 is the index of the semiconductor, θ_1 is the angle of incidence, and θ_2 is the angle of refraction given by Snell's law, $n_1\sin\theta_1 = n_2\sin\theta_2$. For example, for silicon, at a wavelength of 10 μm the refractive index is $n_2=3.4215$. The fraction of the power transmitted for TE or TM polarization is

$$\left(\frac{P_t}{P_i}\right)_{\substack{\text{TE}\\\text{TM}}} = \left(\frac{E_t}{E_i}\right)^2_{\substack{\text{TE}\\\text{TM}}} \frac{n_2}{n_1}\frac{\cos\theta_2}{\cos\theta_1}. \tag{6}$$

The semiconductor exit interface is taken to be parallel to the entrance interface. Under these circumstances, the fraction of the power reflected is the same at this second interface. Thus the slab single-angle plane-wave intensity transmittance is simply the square of the fraction of the power transmitted at the entrance interface, or

$$t_{sl,j} = \left(\frac{P_t}{P_i}\right)^2_{\substack{\text{TE}\\\text{TM}}}, \tag{7}$$

neglecting interference effects between the entrance and exit interfaces. For example, for TE polarized light of wavelength 10 μm at an angle of incidence of 10°, the single-angle plane-wave transmittance of a silicon reference slab is $t_{sl,10}=0.4826$. The reference slab sample may have the same dimensions as that containing the photonic crystal sample. This is typically a first location in a common semiconductor slab that contains both the reference slab and the photonic crystal region. Figure 2(a) depicts incidence upon the reference sample and Fig. 2(b) depicts incidence upon the photonic crystal sample. The "slab" values of the $T_{sl,i}$'s ($T_{sl,50}, T_{sl,40}, T_{sl,30},\ldots,T_{sl,-50}$) are measured using the slab reference sample. These composite transmittances are summations given by

$$\begin{bmatrix} T_{sl,50}\\ T_{sl,40}\\ T_{sl,30}\\ T_{sl,20}\\ T_{sl,10}\\ T_{sl,0}\\ T_{sl,-10}\\ T_{sl,-20}\\ T_{sl,-30}\\ T_{sl,-40}\\ T_{sl,-50} \end{bmatrix} = \begin{bmatrix} a_{40} & a_{30} & a_{20} & 0 & 0 & 0 & a_{20} & a_{30} & a_{40} & 0\\ 0 & a_{40} & a_{30} & a_{20} & 0 & 0 & 0 & a_{20} & a_{30} & a_{40}\\ 0 & 0 & a_{40} & a_{30} & a_{20} & 0 & 0 & 0 & a_{20}+a_{40} & a_{30}\\ 0 & 0 & 0 & a_{40} & a_{30} & a_{20} & 0 & a_{40} & a_{30} & a_{20}\\ 0 & 0 & 0 & 0 & a_{40} & a_{30} & a_{20}+a_{40} & a_{30} & a_{20} & 0\\ 0 & 0 & 0 & 0 & 0 & 2a_{40} & 2a_{30} & 2a_{20} & 0 & 0\\ 0 & 0 & 0 & 0 & a_{40} & a_{30} & a_{20}+a_{40} & a_{30} & a_{20} & 0\\ 0 & 0 & 0 & a_{40} & a_{30} & a_{20} & 0 & a_{40} & a_{30} & a_{20}\\ 0 & 0 & a_{40} & a_{30} & a_{20} & 0 & 0 & 0 & a_{20}+a_{40} & a_{30}\\ 0 & a_{40} & a_{30} & a_{20} & 0 & 0 & 0 & a_{20} & a_{30} & a_{40}\\ a_{40} & a_{30} & a_{20} & 0 & 0 & 0 & a_{20} & a_{30} & a_{40} & 0 \end{bmatrix} \begin{bmatrix} t_{sl,90}\\ t_{sl,80}\\ t_{sl,70}\\ t_{sl,60}\\ t_{sl,50}\\ t_{sl,40}\\ t_{sl,30}\\ t_{sl,20}\\ t_{sl,10}\\ t_{sl,0} \end{bmatrix}. \tag{8}$$

From these measured $T_{sl,i}$'s and from the calculated $t_{sl,j}$'s, the A_{ij}'s (a_{20}, a_{30}, a_{40}) can be determined. This is done by first rewriting Eq. (8) as

$$\begin{bmatrix} T_{sl,50}\\ T_{sl,40}\\ T_{sl,30}\\ T_{sl,20}\\ T_{sl,10}\\ T_{sl,0}\\ T_{sl,-10}\\ T_{sl,-20}\\ T_{sl,-30}\\ T_{sl,-40}\\ T_{sl,-50} \end{bmatrix} = \begin{bmatrix} t_{sl,10}+t_{sl,90} & t_{sl,20}+t_{sl,80} & t_{sl,30}+t_{sl,70}\\ t_{sl,0}+t_{sl,80} & t_{sl,10}+t_{sl,70} & t_{sl,20}+t_{sl,60}\\ t_{sl,10}+t_{sl,70} & t_{sl,0}+t_{sl,60} & t_{sl,10}+t_{sl,50}\\ t_{sl,20}+t_{sl,60} & t_{sl,10}+t_{sl,50} & t_{sl,0}+t_{sl,40}\\ t_{sl,30}+t_{sl,50} & t_{sl,20}+t_{sl,40} & t_{sl,10}+t_{sl,30}\\ 2t_{sl,40} & 2t_{sl,30} & 2t_{sl,20}\\ t_{sl,30}+t_{sl,50} & t_{sl,20}+t_{sl,40} & t_{sl,10}+t_{sl,30}\\ t_{sl,20}+t_{sl,60} & t_{sl,10}+t_{sl,50} & t_{sl,0}+t_{sl,40}\\ t_{sl,10}+t_{sl,70} & t_{sl,0}+t_{sl,60} & t_{sl,10}+t_{sl,50}\\ t_{sl,0}+t_{sl,80} & t_{sl,10}+t_{sl,70} & t_{sl,20}+t_{sl,60}\\ t_{sl,10}+t_{sl,90} & t_{sl,20}+t_{sl,80} & t_{sl,30}+t_{sl,70} \end{bmatrix} \begin{bmatrix} a_{40}\\ a_{30}\\ a_{20} \end{bmatrix}. \tag{9}$$

Then the intensity weighting coefficients, a_{20}, a_{30}, a_{40}, may be determined using the method described in the next section.

IV. INTENSITY WEIGHTING COEFFICIENTS

The linear equations represented by Eq. (9) are an overdetermined set of equations. There are more equations (M) than unknowns (N). This is due to making more measurements than the minimum needed to determine the intensity weighting coefficients. The larger number of measurements is desirable to compensate for noise in the measured composite transmittances (T's) and thus to improve the overall accuracies of the intensity weighting coefficients. The issue is how to use all the measured information that is available to obtain the most accurate set of answers (a's) possible. A widely used strategy[23] is to define the error vector e as $e = t_{sl}a - T_{sl}$ and to minimize $\Sigma_i |e_i|^2$. The resulting solution that minimizes the squared error is

$$a = (t_{sl}^T t_{sl})^{-1} t_{sl}^T T_{sl}, \tag{10}$$

where t_{sl} is the coefficient matrix of Eq. (9), t_{sl}^T is the transpose of t_{sl}, and $(*)^{-1}$ represents the matrix inverse. The quantity $(t_{sl}^T t_{sl})^{-1} t_{sl}^T$ is the Moore–Penrose matrix inverse of t_{sl}. It is also referred to as the ''generalized inverse'' or ''pseudoinverse.''[23]

V. COMPOSITE TRANSMITTANCES OF PHOTONIC CRYSTAL SAMPLE

Next, the silicon slab containing the photonic crystal sample is translated into position as shown in Fig. 2(b). It should have the same external dimensions as the previous blank silicon reference slab. In fact, it may be a second location on the same silicon sample. Now the composite transmittances $T_{pc,i}$ are measured over a range of objective-sample angles of incidence. These composite transmittances are related to the unknown single-angle plane-wave transmittances by

$$\begin{bmatrix} T_{pc,50} \\ T_{pc,40} \\ T_{pc,30} \\ T_{pc,20} \\ T_{pc,10} \\ T_{pc,0} \\ T_{pc,-10} \\ T_{pc,-20} \\ T_{pc,-30} \\ T_{pc,-40} \\ T_{pc,-50} \end{bmatrix} = \begin{bmatrix} a_{40} & a_{30} & a_{20} & 0 & 0 & 0 & a_{20} & a_{30} & a_{40} & 0 \\ 0 & a_{40} & a_{30} & a_{20} & 0 & 0 & 0 & a_{20} & a_{30} & a_{40} \\ 0 & 0 & a_{40} & a_{30} & a_{20} & 0 & 0 & 0 & a_{20}+a_{40} & a_{30} \\ 0 & 0 & 0 & a_{40} & a_{30} & a_{20} & 0 & a_{40} & a_{30} & a_{20} \\ 0 & 0 & 0 & 0 & a_{40} & a_{30} & a_{20}+a_{40} & a_{30} & a_{20} & 0 \\ 0 & 0 & 0 & 0 & 0 & 2a_{40} & 2a_{30} & 2a_{20} & 0 & 0 \\ 0 & 0 & 0 & 0 & a_{40} & a_{30} & a_{20}+a_{40} & a_{30} & a_{20} & 0 \\ 0 & 0 & 0 & a_{40} & a_{30} & a_{20} & 0 & a_{40} & a_{30} & a_{20} \\ 0 & 0 & a_{40} & a_{30} & a_{20} & 0 & 0 & 0 & a_{20}+a_{40} & a_{30} \\ 0 & a_{40} & a_{30} & a_{20} & 0 & 0 & 0 & a_{20} & a_{30} & a_{40} \\ a_{40} & a_{30} & a_{20} & 0 & 0 & 0 & a_{20} & a_{30} & a_{40} & 0 \end{bmatrix} \begin{bmatrix} t_{pc,90} \\ t_{pc,80} \\ t_{pc,70} \\ t_{pc,60} \\ t_{pc,50} \\ t_{pc,40} \\ t_{pc,30} \\ t_{pc,20} \\ t_{pc,10} \\ t_{pc,0} \end{bmatrix}, \tag{11}$$

which has the same coefficient matrix as Eq. (8). Now, however, the a's are known quantities. Thus the t_{pc}'s can be determined. In this simplified representation depicted in Eq. (11), there are 11 measured values of $T_{pc,i}$ ($T_{pc,-50},\ldots,T_{pc,0},\ldots,T_{pc,50}$) and ten unknown values of $t_{pc,j}$ ($t_{pc,0},t_{pc,10},\ldots,t_{pc,90}$). In general, there are M measurements extending from $-\theta_{s,\max}$ to $+\theta_{s,\max}$. If the angular step size is $\Delta\theta_s$, then the number of measurements is

$$M = 2\frac{\theta_{s,\max}}{\Delta\theta_s} + 1. \tag{12}$$

The unknown single-angle plane-wave transmittances of the photonic crystal structure are for angles from $\theta_k = 0$ to $\theta_k = \theta_{k,\max}$ where $\theta_{k,\max} = \theta_{s,\max} + \theta_{\mathrm{ob,max}}$ [Eq. (4)]. The maximum plane wave angle of incidence, $\theta_{k,\max}$, present in the measurement, of course, is typically less than 90°. The number of unknown single-angle plane-wave transmittances, N, is

$$N = \frac{\theta_{s,\max} + \theta_{\mathrm{ob,max}}}{\Delta\theta_k} + 1. \tag{13}$$

Using Eqs. (12) and (13), typical values of the number of composite transmittance measurements (M) and number of unknown single-angle plane-wave transmittances (N) are given in Table II for various values of the angular resolution in angular measurement ($\Delta\theta_s$) and the angular separation between the single-angle plane-wave transmittances ($\Delta\theta_k$). The practical case of $\Delta\theta_s = \Delta\theta_k/2$ is included in Table II. This corresponds to making two measurements in each angular range equal to the angular separation between the values of the plane-wave transmittances to be calculated. Noninteger values may arise from Eqs. (12) and (13), but of course only integer numbers of measurements and unknowns exist. When $\theta_{\mathrm{ob,max}} = \theta_{s,\max}$ and $\Delta\theta_s = \Delta\theta_k$, the number of measurements (M) and the number of unknowns (N) are the same.

VI. SINGLE-ANGLE PLANE-WAVE TRANSMITTANCES OF PHOTONIC CRYSTAL SAMPLE

The linear equations represented by Eq. (11) are again an overdetermined set of equations. This is due to making more measurements than the minimum needed to determine the single-angle plane-wave transmittances. This reduces the effects of experimental noise. As before, the optimum solution that minimizes the squared error is given in terms of the Moore–Penrose matrix inverse. The resulting solution is

$$t_{pc}=(A^TA)^{-1}A^TT_{pc}, \tag{14}$$

where A is the coefficient matrix of Eq. (11), A^T is the transpose of A, and $(*)^{-1}$ represents the matrix inverse. In this fashion, the single-angle plane-wave transmittances of the photonic crystal sample may be determined.

VII. DISCUSSION

In summary, the complete procedure for determining the single-angle plane-wave transmittances of the photonic crystal sample for a given wavelength and a given polarization (either TE or TM) may be described as follows: (1) Install a horizontal slit before the objective to limit angles of incidence to the horizontal plane. (2) Calculate, based on the Fresnel equations or other electromagnetic method, the single-angle plane-wave transmittances, $t_{sl,i}$'s (e.g., $t_{sl,0}$, $t_{sl,10}$, $t_{sl,20}$, etc.) taking into account reflections at the entrance surface and at the exit surface [Eq. (7)]. (3) Insert the reference semiconductor slab sample aligned with the horizontal slit. This is typically the first location on a common slab sample that contains the reference region as the first location [Fig. 2(a)] and the photonic crystal sample as the second location [Fig. 2(b)]. (4) Measure the composite transmittances $T_{sl,i}$'s (e.g., $T_{sl,0}$, $T_{sl,10}$, $T_{sl,20}$, etc.) of the reference semiconductor slab over a range of objective-sample angles of incidence. (5) Calculate, using the Moore–Penrose matrix inversion method, the objective intensity-angular-weighting coefficients a's (e.g., a_{10}, a_{20}, a_{30}, etc.) from Eq. (10). (6) Translate the photonic crystal semiconductor sample into the focal region [Fig. 2(b)]. (7) Measure the composite transmittances $T_{pc,i}$'s (e.g., $T_{pc,0}$, $T_{pc,10}$, $T_{pc,20}$, etc.) of the photonic crystal sample over a range of objective-sample angles of incidence. (8) Using the a's from the reference semiconductor slab measurement, calculate, using the Moore–Penrose matrix inversion method, the single-angle plane-wave photonic crystal transmittances $t_{pc,j}$'s (e.g., $t_{pc,0}$, $t_{pc,10}$, $t_{pc,20}$, etc.) from Eq. (14). This procedure applies to a single wavelength and a single polarization. To obtain the spectral characterization of the photonic crystal sample, this procedure needs to be repeated for each wavelength of interest. This can be done one wavelength at a time by changing the wavelength of a tunable source or by using a simultaneous range of wavelengths as done in conjunction with an FTIR spectrometer. To set the linear polarization an infrared polarizer in the optical system may be rotated to select either TE or TM polarization.

TABLE II. The number of measurements (composite transmittances), M, and the number of unknowns (single-angle plane-wave transmittances), N, as a function of $\theta_{\mathrm{ob,max}}$, $\theta_{s,\mathrm{max}}$, $\Delta\theta_s$, and $\Delta\theta_k$.

$\theta_{\mathrm{ob,max}}$ (deg)	$\theta_{s,\mathrm{max}}$ (deg)	$\Delta\theta_s$ (deg)	M (T's)	$\Delta\theta_k$ (deg)	N (t's)
30	40	0.5	161	1	71
30	40	1	81	1	71
30	40	1	81	2	36
30	40	2	41	2	36
30	40	2.5	33	5	15
30	40	5	17	5	15
30	40	5	17	10	8
30	40	10	9	10	8
40	50	0.5	201	1	91
40	50	1	101	1	91
40	50	1	101	2	46
40	50	2	51	2	46
40	50	2.5	41	5	19
40	50	5	21	5	19
40	50	5	21	10	10
40	50	10	11	10	10

A powerful benefit of obtaining the resulting single-angle plane-wave transmittances of the photonic crystal sample obtained as described here, is that these experimentally based single-angle plane-wave transmittances can be compared to values calculated theoretically using the plane-wave expansion method or the finite-difference time-domain (FDTD) method. In photonic crystal device development, this information is invaluable in assessing device performance and in reconciling differences among analysis, design, fabrication, and testing of these devices. The above methodology has been developed in terms of transmittances. However, as stated previously, it also applies to single-angle plane-wave reflectance determination. Likewise, the approach can be applied to measurement with refractive lenses. In this case, the same formulation is used except that $\theta_{\mathrm{ob,min}}=0$. Further, this approach can be applied equally to 1D, 2D, and 3D photonic crystal structures. Although the formulation has been developed for symmetrical beams and symmetrical samples [Eq. (3)], this approach can be reformulated to incorporate nonsymmetrical cases. The methodology presented here can be straightforwardly implemented using MATLAB[24] or similar software packages.

ACKNOWLEDGMENT

This research was supported in part by Grant No. DAAD19-03-1-0286 from the Army Research Office.

[1] J. D. Joannopoulos, R. D. Meade, and J. N. Winn, *Photonic Crystals* (Princeton University Press, Princeton, NJ, 1995).
[2] E. Yablonovitch, Phys. Rev. Lett. **58**, 2059 (1987).
[3] S. John, Phys. Rev. Lett. **58**, 2486 (1987).
[4] U. Gruning, V. Lehmann, and C. M. Engelhardt, Appl. Phys. Lett. **66**, 3254 (1995).
[5] M. Wada, Y. Doi, K. Inoue, J. W. Haus, and Z. Yuan, Appl. Phys. Lett. **70**, 2966 (1997).
[6] S. Rowson, A. Chelnokov, J. M. Lourtioz, and F. Carcenac, J. Appl. Phys. **83**, 5061 (1998).
[7] P. Bhattacharya, W. Zhou, D. Zhu, and J. Sabarinathan, Appl. Phys. Lett. **75**, 1670 (1999).
[8] F. Genereux, S. W. Leonard, H. M. van Driel, A. Birner, and U. Gosele, Phys. Rev. B **63**, 161101 (2001).
[9] Y. Xu, H. B. Sun, J. Y. Ye, S. Matsuo, and H. Misawa, J. Opt. Soc. Am. B **18**, 1084 (2001).
[10] J. Schilling, A. Birner, F. Muller, R. B. Wehrspohn, R. Hillebrand, U.

Gosele, K. Busch, S. John, S. W. Leonard, and H. M. van Driel, Opt. Mater. (Amsterdam, Neth.) **17**, 7 (2001).
[11] H. Hatate, M. Hashimoto, H. Shirakawa, Y. Fujiwara, Y. Takeda, H. Nakano, T. Tatsuta, and O. Tsuji, Jpn. J. Appl. Phys., Part 1 **37**, 7172 (1998).
[12] S. Rowson, A. Chelnokov, C. Cuisin, and J. M. Lourtioz, IEE Proc.: Optoelectron. **145**, 403 (1998).
[13] S. Rowson, A. Chelnokov, and J. M. Lourtioz, J. Lightwave Technol. **17**, 1989 (1999).
[14] S. Rowson, A. Chelnokov, C. Cuisin, and J. M. Lourtioz, J. Opt. A, Pure Appl. Opt. **1**, 483 (1999).
[15] M. Galli, M. Agio, L. C. Andreani, M. Belotti, G. Guizzetti, F. Marabelli, M. Patrini, P. Bettotti, L. Dal Negro, Z. Gaburro, L. Pavesi, A. Lui, and P. Bellutti, Phys. Rev. B **65**, 113111 (2002).
[16] P. Kramper, A. Birner, M. Agio, C. M. Soukoulis, F. Muller, U. Gosele, J. Mlynek, and V. Sandoghdar, Phys. Rev. B **64**, 233102 (2001).
[17] A. Birner, U. Gruning, S. Ottow, A. Schneider, F. Muller, V. Lehmann, H. Foll, and U. Gosele, Phys. Status Solidi: A **165**, 111 (1998).
[18] A. Birner, A. P. Li, F. Muller, U. Gosele, P. Kramper, V. Sandoghdar, J. Mlynek, K. Busch, and V. Lehmann, Mater. Sci. Semicond. Process. **3**, 487 (2000).
[19] S. W. Leonard, H. M. van Driel, K. Busch, S. John, A. Birner, A. P. Li, F. Muller, U. Gosele, and V. Lehmann, Appl. Phys. Lett. **75**, 3063 (1999).
[20] G. R. Kilby and T. K. Gaylord, Opticol Society of Amarica Annual Meeting, TuE6, 2003 (unpublished).
[21] Thermo-Oriel, 150 Long Beach Blvd., Stratford, CT 06615.
[22] Ealing Inc., 3845 Atherton Road, Rocklin, CA 95765.
[23] G. Strang, *Linear Algebra and Its Applications*, 2nd ed. (Academic, New York, 1980).
[24] MathWorks Inc., 24 Prime Park Way, Natick, MA 01760.